Astron. Nachr. / AN **337**, No. 10, 1045 – 1049 (2016) / **DOI** 10.1002/asna.201612431

NLTE modeling of a small active region filament observed with the VTT

P. Schwartz[1,⋆], **H. Balthasar**[2], **C. Kuckein**[2], **J. Koza**[1], **P. Gömöry**[1], **J. Rybák**[1], **P. Heinzel**[3], and **A. Kučera**[1]

[1] Astronomical Institute, Slovak Academy of Sciences, SK-05960 Tatranská Lomnica, Slovak Republic
[2] Leibniz-Institut für Astrophysik Potsdam (AIP), An der Sternwarte 16, D-14482 Potsdam, Germany
[3] Astronomical Institute, Academy of Sciences of the Czech Republic, Fričova 298, CZ-25165 Ondřejov, Czech Republic

Received 2016 Aug 31, accepted 2016 Sep 02
Published online 2016 Dec 02

Key words Sun: filaments, prominences – Sun: infrared – techniques: polarimetric – techniques: spectroscopic – radiative transfer

An active region mini-filament was observed with the Vacuum Tower Telescope (VTT) in Tenerife simultaneously in the He I infrared triplet using the Tenerife Infrared Polarimeter 1 (TIP 1), in Hα with the TESOS Fabry-Pérot interferometer, and in Ca II 8542 Å with the VTT spectrograph. The spectropolarimetric data were inverted using the HAZEL code and Hα profiles were modelled by solving a NLTE radiative transfer in a simple isobaric and isothermal 2D slab irradiated both from its bottom and sides from the solar surface. It was found that the mini-filament is composed of horizontal fluxtubes, along which the cool plasma of $T \sim 10\,000$ K can flow with very large, even supersonic, velocities.

1 Introduction

Filaments are on-disk manifestations of relatively cool and dense plasma structures hovering in the corona with roots in the low atmosphere. The typical length of filaments is ranging from 60 to 600 Mm (Tandberg-Hanssen 1995). In this study we focus on a small filament with the length below 60 Mm occurring at the periphery of an active region. Such objects are largely unexplored and often overlooked. Denker & Tritschler (2009) called them "mini-filaments", and we use this term throughout this study. These small and very dynamic structures in active regions were examined in more detail in Sterling et al. (2015). In this work we combine multispectral and specropolarimetric observations of the mini-filament with its Hα spectral imagery to infer its magnetic and thermodynamic structure.

2 Observations

A mini-filament in the NOAA 12159 active region was observed on 2014 September 11 from 9:28 to 10:04 UT at the Vacuum Tower Telescope (VTT) in Tenerife. Observations were carried out simultaneously in the infrared helium triplet with the Tenerife Infrared Polarimeter 1 (TIP 1; Martínez Pillet et al. 1999) attached to the Echelle spectrograph and in Hα with the Triple Etalon SOlar Spectrometer (TESOS; Tritschler et al. 2002). The HMI line-of-sight (LOS) magnetogram in the top panel of Fig. 1 shows that the left part of the target area involves a patchy and sparse plage with a few pores as seen in the HMI continuum image (not shown here). The target filament, seen in the GONG Hα broad-band image shown in the bottom panel of the figure, looks as an elongated structure centered at $(x, y) = (+215'', -420'')$ and anchored at the edge of the plage. Nevertheless, it is occupying mostly a non-magnetic area. Therefore its nature is imaginable only as a single magnetic fluxtube or a bundle of fluxtubes interconnecting areas of opposite polarities.

Spectropolarimetric observations in full Stokes in the He I infrared triplet with wavelengths around 10 830 Å were obtained with TIP 1. Three small scans ($\approx 10''$ wide) were taken using the reflective beam splitter of the adaptive optics. The slit length corresponded to $30''$ and one step of the scanning was set to $0\farcs45$. We acquired four modulation stages with 50 ms exposures each. To increase signal-to-noise ratio of the recorded Stokes parameters, we summed 40 sets of the modulation states at each scan position. Using this summation, a total integration time of 8 s and a cadence of approximately 10 s between two consecutive scanning positions was yielded. Together with the spectropolarimetry, also spectroscopic observations in the Ca II 8542 Å line were obtained at the spectrograph. The third scan taken between 09:56:28 and 10:04:43 UT was chosen for the further analysis because of the best quality. With TESOS we took 2D images with a field of view (FOV) of $25''\times25''$ in 136 wavelength points through the Hα profile within the wavelength interval 6561.17 – 6564.48 Å ($\Delta\lambda$ = 24.5 mÅ). TESOS made 35 of such scans during the spectrograph observations. The simultaneously obtained white-light (WL) images of TESOS were used to correct for seeing and pointing effects during the Hα line scanning. The scan 33 of TESOS was least affected by seeing and therefore taken for further analysis.

⋆ Corresponding author: pschwartz@astro.sk

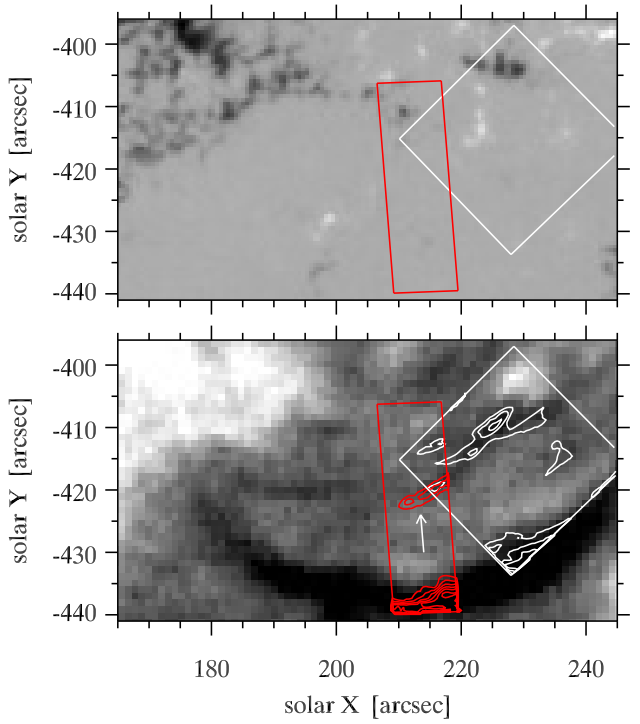

Fig. 1 *Top*: the HMI LOS magnetogram of the target area taken on 2014 September 11 at 10:01:20 UT. *Bottom*: the Hα image of the same area from the NSO/GONG Hα network monitor (Harvey et al. 2011) at the Teide Observatory taken at 10:01:14 UT. The filament visible at the bottom panel occurred at the south edge of active region NOAA 12159. The white square defines the FOV of TESOS and the red rectangle identifies the area of TIP 1 scan 3. The arrow marks the mini-filament studied in this work.

All observed data were corrected by standard methods, such as dark-frame subtraction, flat-fielding, and correction for image deformations. Then they were aligned and compensated for pointing and seeing effects. All these data handling tasks were performed extensively profiting from the SolarSoft System (Freeland & Handy 1998) and for the TESOS data the `TESOS_LIB` IDL library (Schleicher & Schlichenmaier 2007) has also been used. The spectropolarimetric data were also corrected for effects of instrumental polarisation and cross-talk (see Collados 2003 and references therein). For the radiometric calibration of TESOS Hα profiles, disc-center observations and the atlas of Neckel (1999) were used. Finally, the Hα profiles were smoothed by the Savitzky-Golay filter that generally preserves depths and widths of line profiles (Press et al. 1992).

The spatial co-alignment of the TIP 1, TESOS, and Ca II 8542 Å datasets was accomplished using the HMI continuum image. Granulation in the target area seen in the HMI image served us as a framework to identify common granulation patterns in the intensity maps obtained with TIP 1 in continuum close to the He triplet, with the Echelle spectrograph in the far wing of the Ca II line and in the WL images from TESOS. The TIP 1 and TESOS FOVs, co-aligned and correctly oriented according to solar North, are shown in Fig. 2.

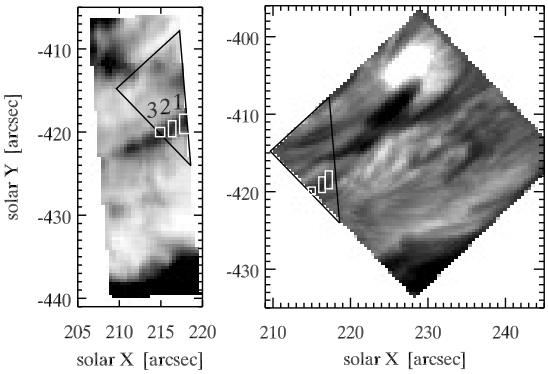

Fig. 2 *Left*: the slit-reconstructed monochromatic image of the target area in the line center of the red component of the He I 10830 Å triplet observed by TIP 1. The scanning ran from 09:56:28 UT to 10:04:43 UT. *Right*: the Hα line center image of the target taken by TESOS at 10:01:33 UT. The black lines identify a triangular overlap area of TIP 1 and TESOS FOVs. White lines mark three rectangular segments at the mini-filament selected for an analysis.

3 Method

3.1 HAZEL inversion

The HAZEL code (Asensio Ramos et al. 2008) is used for synthesis and inversion of Stokes profiles of several spectral lines of helium (e.g., He I IR triplet, D3, etc.) solving the detailed radiative transfer in the 1D geometry taking into account atomic level polarisation and Zeeman, Hanle, and Paschen-Back effects. In the model, a slab with constant properties illuminated asymmetrically from below is assumed. For the irradiation of the slab, the center-to-limb variation is taken into account. We used the code in the mode of one optically thick slab. The slab is situated in the height h above the solar surface in a presence of a deterministic magnetic field of arbitrary strength, inclination and azimuth. The influence of the LOS velocity $v_{\rm LOS}$ of the slab plasma on the resulting profiles is included. More details about the theory of radiative transfer of polarised radiation applied in the code can be found in Trujillo Bueno & Asensio Ramos (2007).

3.2 A simple cloud modeling

Mostly, the optical thickness of solar prominences and filaments in Hα and the IR lines of singly ionised calcium is small (not exceeding much the unity). Thus, source function in such structures illuminated from the disk can be assumed being independent on optical depth and wavelength (see, e.g., review of Heinzel 2015). This type of modelling is then called as the cloud model and solution of radiative transfer simplifies as follows: The constant source function in the formal solution of the radiative transfer (see Mihalas 1978) can be taken out of the integral, and then the intensity can be calculated analytically as shown in Schwartz et al. (2015) for prominences. Unlike in the case of prominences,

for filaments also the background radiation decreased by an absorption must be added to the emerging intensity. The cloud model in 1D geometry was fitted to the observed profiles using the Levenberg-Marquardt method. The Doppler width $\Delta\lambda_D$ depends on temperature divided by the weight of the ion and on the microturbulence velocity v_{MT} (see Schwartz et al. 2015). Sensitivity of $\Delta\lambda_D$ on temperature and on v_{MT} are comparable for Hα. Thus, first v_{MT} is derived from $\Delta\lambda_D$ of the Ca II 8542 Å line because it is much less sensitive to temperature as the calcium atom is approximately forty times heavier than the atom of hydrogen. Then this microturbulence velocity is used to derive the temperature from the Doppler width obtained from the cloud-model fitting of the Hα profiles.

3.3 2D NLTE modeling

The Hα line profiles observed at the mini-filament were modelled using a simple 2D NLTE model. It was assumed that the mini-filament is composed of multiple fluxtubes placed one above another. The filament plasma is flowing inside them along the magnetic field. For the simple 2D model used in this work, a system of fluxtubes is approximated by the isothermal and isobaric 2D slab of a box-like cross-section with two finite dimensions – vertical Z and across the filament X. The dimension Y along the filament is infinite and inclined by an angle of 18° from the direction to the solar West. The width of the dark structure of the mini-filament of 1000 km was measured in the Hα center intensity map (right panel of Fig. 2) and was used as the X dimension of the slab. The vertical height (Z dimension) together with temperature and plasma pressure were taken as free parameters of the model. The slab is irradiated at its bottom and sides from the solar surface and it is situated in the height h above it.

The radiative transfer in the 2D model is solved using the short-characteristics method (Kunasz & Auer 1988) together with the Multilevel Accelerated Lambda Iterations (MALI) (Rybicki & Hummer 1991). The 2D code used in this study is described in Heinzel & Anzer (2001) and was accordingly modified to account for a filament geometry. The statistical equilibrium was calculated for a 5-level plus continuum hydrogen atom. The formal solution of the radiative transfer was made along the LOS at $\mu = 0.87$ corresponding to the position of the mini-filament on the solar disc. It is assumed that plasma flows along the fluxtubes, and this flow is oriented along the filament dark structure. The angle of the flow inclination from the vertical Z is taken as a free parameter. We assumed that very broad Hα profiles observed at the mini-filament can be emitted only by a system of multiple fluxtubes in which plasma is flowing with different, even opposite, velocities. We approximated such a system of fluxtubes by two isothermal and isobaric 2D slabs with opposite plasma-flow velocities contributing to emerging radiation by a filling factor of 0.5.

Table 1 Minimum and maximum values of parameters inferred from the cloud-model fitting of the profiles from the three segments of the mini-filament. The source function S is expressed in 10^{-6} erg cm^{-2} s^{-1} sr^{-1} Hz^{-1}. The quantities T, $\Delta\lambda_D$, τ_{6563}, v_{LOS}, and v_{MT} are temperature, Doppler width of Hα, optical thickness in the Hα line center, line-of-sight velocity, and microturbulence velocity, respectively.

Parameter	Seg. 1	Seg. 2	Seg. 3
S	2.55 – 4.71	2.92 – 3.68	2.98 – 3.52
T [kK]	34.2 – 49.1	31.8 – 39.7	20.3 – 31.8
$\Delta\lambda_D$ [Å]	0.53 – 0.63	0.53 – 0.63	0.45 – 0.54
τ_{6563}	0.41 – 0.78	0.42 – 0.77	0.62 – 0.87
v_{LOS} [km s^{-1}]	−1.1 – +2.4	−4.7 – +0.5	−3.5 – −2.1
v_{MT} [km s^{-1}]	3.7 – 6.0	4.6 – 14.4	6.7 – 11.9

Table 2 Properties inferred for the three segments at the mini-filament by the 2D NLTE modeling of the observed Hα profiles. The inclination is an angle between local vertical and fluxtubes comprised in the slab.

Height of slab base	9 000–13 000 km
Slab width	1 000 km
Slab vertical thickness	60 000 km
Inclination	90–100°
Temperature	9 000 K
Pressure	0.12 dyn cm^{-2}
Flow velocity	±25 km s^{-1}
Microturbulence	5–13 km s^{-1}

4 Results

An attempt to estimate the magnetic field vector from the spectropolarimetric observations of the He I 10830 Å triplet was made using the HAZEL (Asensio Ramos et al. 2008) inversion code. Due to a very low signal-to-noise ratio in Q and U profiles, resulting values of the magnetic field azimuth and inclination were affected by huge uncertainties and therefore not usable. At least, it was possible to reliably fit the intensity profiles and obtain optical thickness in the center of the red component of the He I triplet and LOS velocities v_{LOS}. Maps of the optical thickness and v_{LOS} obtained from the inversion of the intensity profiles are shown in Fig. 3. An increase of the optical thickness is well pronounced in the dark structure of the mini-filament. The values of v_{LOS} estimated there are almost zero not exceeding the interval ±1 km s^{-1}. Contrary to that, areas with more significant downflows and upflows (although not exceeding several km s^{-1}) are located northward and southward of the dark structure, respectively.

Three segments at dark structure of the mini-filament were chosen within the overlapping area the of FOVs of TIP 1 and TESOS during scan 3 as marked in Fig. 2. The Ca II 8542 Å and Hα profiles from different positions within the three segments were fitted by the simple cloud model (see Sect. 3.2). Averaged profiles from the quiet-Sun (QS) area northward from the dark structure were used as the background irradiation. An example of fitting the Hα profile

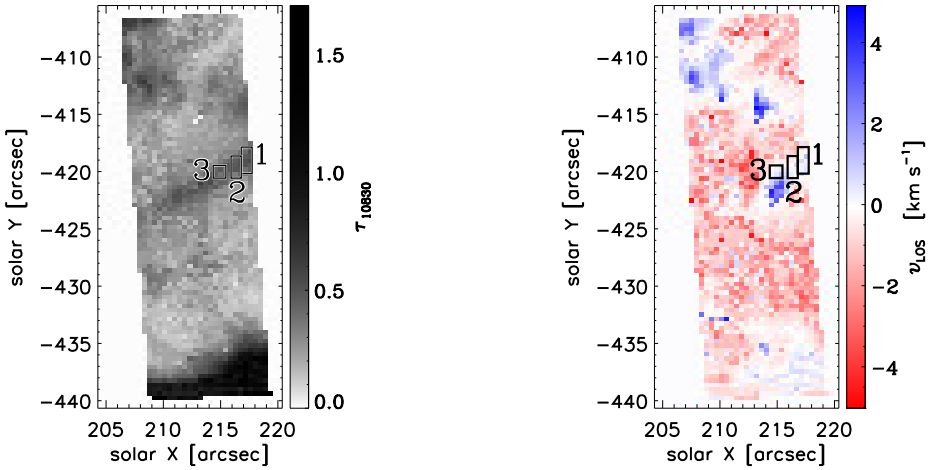

Fig. 3 The optical thickness at center of the red component of the He I IR triplet τ_{10830} (*left*) and the line-of-sight velocities v_{LOS} (*right*) inferred by the HAZEL inversion of intensity profiles of the He I IR triplet. Positive values of v_{LOS} correspond to blueshift, negative to redshift.

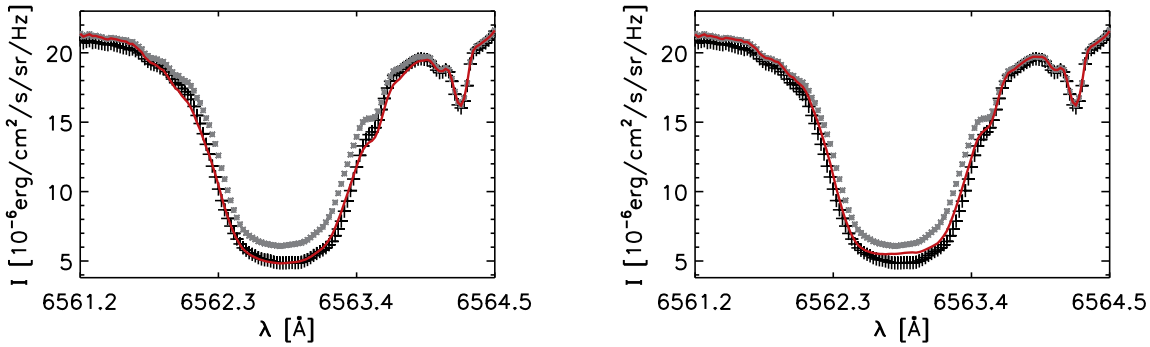

Fig. 4 Examples of comparison of the observed (plus signs) and synthetic (solid red line) Hα profiles from the segment 1 of the dark structure of the mini-filament at position (+217″, −419″) resulting from the simple cloud-model fitting (*left*) and NLTE 2D modelling (*right*). The observed profile from the quiet-Sun area is plotted by gray asterisks.

observed at the dark structure is shown in the left panel of Fig. 4. Intervals of resulting parameters of the cloud-model fitting are listed in Table 1. Although values of the optical thickness τ_{6563} at the Hα center are rather small for a filament – not exceeding unity, still more than 30 % of background radiation is absorbed ($\tau_{6563} > 0.4$). The LOS velocities v_{LOS} are very low – their absolute values do not exceed several km s^{-1}. Temperatures of 20–50 kK are too high for the Hα line formation and therefore not realistic. Such unrealistic results – large Doppler widths (and subsequently very high temperatures) together with very small v_{LOS} velocities – indicate that horizontal plasma flows of large velocities must be present in the mini-filament.

With a trial-and-error method, we searched for the NLTE model that fits best the Hα profiles observed in the dark structure of the mini-filament in the three segments. We varied the temperature between 6 000 and 15 000 K and plasma pressure within 0.08–0.2 dyn cm^{-2}. For each model, the synthetic Hα profiles emerging from the X and Z grid-points on the surface of the 2D slab for μ equal to 0.87 were compared with the observed profiles. Finally, the synthetic profile which best fitted the observed one was chosen.

Parameters of the best models are listed in Table 2. High velocities of plasma flows and very large vertical size of the slab had to be chosen to fit very broad and deep observed Hα profiles. Despite of the large vertical size, the optical thickness of the slab in the Hα center does not exceed 0.6. This can be explained by remarkable inclination of LOS from the vertical as shown in Fig. 5 what shortens much geometrical thickness of the slab along LOS. Plasma flows must be almost perpendicular to LOS in order to get very small v_{LOS} values as obtained from the HAZEL inversions of the He I IR triplet. An example of the comparison of the Hα profile observed in the segment 1 with the best synthetic profile is shown in the right panel of Fig. 4. The NLTE modelling shown that the very deep Hα profiles observed in all three segments in the dark structure originate from a very bottom part of the slab. In Fig. 5 it is shown how LOS is passing through the slab in this case. Because of rather large inclination of LOS from the vertical, emission from a very bottom part of the slab is not totally absorbed as it would be in the case of vertically directed LOS (along the Z dimension of the slab). In the other hand, much shallower profiles observed at a brighter area adjacent from South to the dark

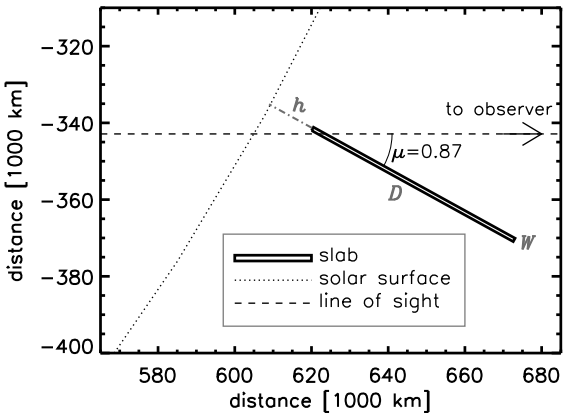

Fig. 5 Geometry of the 2D slab viewed from a side according to results from the NLTE 2D modelling (Table 2). The slab is situated radially in height h, its width is W and vertical thickness D. Distances from the Sun center is shown on the axes. Position of the mini-filament remarkably away from the disk center causes that beams of LOS intersects the slab at angle of $\mu = 0.87$ from the vertical. The beam for the darkest part of the mini-filament is shown.

structure were fitted well by the synthetic profiles radiated out from higher parts of the 2D slab. A remarkable feature of the resulting slab model is its capability to explain subtle intensity variations observed across the mini-filament. A distribution of the observed Hα core intensities along a cut made perpendicularly to the main axis of the mini-filament at the position $X = 217''$ shows subtle brightenings. They are well reproduced by the computed line core intensities synthesized along the slab. This enhances the plausibility of our slab model. It also means that both the dark structures and brighter areas between them, as it is visible in the right panel of Fig. 2, belong to the same mini-filament.

5 Conclusion

Very deep and broad Hα profiles were observed at the dark structure of a small active region filament. They were modelled using NLTE radiative transfer in an isobaric and isothermal 2D slab irradiated both from the bottom and sides. It was assumed that the filament is composed of multiple horizontal fluxtubes. The fluxtubes contain a rather cool plasma of a temperature of $\sim 10\,000$ K, pressure 0.12 dyn cm^2, density of $1.5{\times}10^{-13}$ g cm^{-3} and degree of ionisation of hydrogen around 0.4 typical for solar prominences/filaments. The speed of sound of 11.6 km s^{-1} corresponds to such temperature and ionisation degree. The plasma flows along the fluxtubes with very large velocities up to 25 km s^{-1} which are supersonic for the estimated temperature and ionisation degree. Even this simple 2D slab-model without any fine structures can reproduce small filamentary objects similar to those observed in Hα, composed of dark mini-filaments and brighter areas in between.

Acknowledgements. This work was supported by the Slovak Research and Development Agency under the contract No. APVV-0816-11 and by the Science Grant Agency project VEGA 2/0004/16. It was made in the frame of the collaboration between the Slovak Academy of Sciences and the Leibniz-Institut für Astrophysik Potsdam (AIP) supported by the Deutscher Akademischer Austauschdienst, project No. 57065721. This article was created by the realisation of the project ITMS No. 26220120009, based on the supporting operational Research and development program financed from the European Regional Development Fund. SDO HMI data are provided by the Joint Science Operations Center – Science data Processing. The GONG network is carried out in the frame of the Integrated Synoptic Program of the National Solar Observatory. The Vacuum Tower Telescope (VTT) in Tenerife is operated by the Kiepenheuer-Institut für Sonnenphysik (Germany) at the Spanish Observatorio del Teide of the Instituto de Astrofísica de Canarias. The observations of VTT used in this work were taken within the EU-7RP-SOLARNET Transnational Access and Service Programme (Ref. nr.: VTT 14-08).

References

Asensio Ramos, A., Trujillo Bueno, J., & Landi Degl'Innocenti, E. 2008, ApJ, 683, 542
Collados, M. 2003, in Polarimetry in Astronomy, ed. S. Fineschi, Proc. SPIE, Vol. 4843
Denker, C., & Tritschler, A. 2009, in Cosmic Magnetic Fields: From Planets, to Stars and Galaxies, eds. Strassmeier, K.G., Kosovichev, A.G., & Beckman, J.E., IAU Symp. Vol. 259, 223
Harvey, J. W., Bolding, J., Clark, R., et al. BAAS, Vol. 43, 17.45
Heinzel, P., & Anzer, U. 2001, A&A, 375, 1082
Heinzel, P. 2015, Ap&SS Library, Vol. 415, p. 110
Freeland, S. L., Handy, B. N. 1998, Sol. Phys., 182, 497
Kunasz, P., Auer, L. H. 1988, J. Quant. Spec. Radiat. Transf., 39, 67
Martínez Pillet, V., Collados, M., Sánchez Almeida, J., et al. 1999, ASP Conf. Ser., 183, 264
Mihalas, D. 1978, Stellar atmospheres, 2nd edition (San Francisco, W. H. Freeman and Co.)
Neckel, H. 1999, Sol. Phys., 184, 421
Press, W. H., Teukolsky, S. A., Vetterling, W. T., Flannery, B. P. 1992, Numerical Recipes in C. The Art of Scientific Computing (Cambridge: University Press, 2nd ed.)
Rybicki, G. B., & Hummer, D. G. 1991, A&A, 245, 171
Schleicher, H., & Schlichenmaier, R. 2007, `TESOS_LIB` User Manual, priv. commun.
Schwartz, P., Heinzel, P., Kotrč, P., et al. 2015, A&A, 574, A62
Sterling, A.C., Moore, R.L., Falconer, D.A., & Adams, M. 2015, Nature, 523, 437
Tandberg-Hanssen, E. 1995, The Nature of Solar Prominences, Ap&SS Library, Vol. 199
Tritschler, A., Schmidt, W., Langhans, K., & Kentischer, T. 2002, Sol. Phys., 211, 17
Trujillo Bueno, J., & Asensio Ramos, A. 2007, ApJ, 655, 642